

## Ratio of the Formation Cross Sections of $^{44g}\text{Sc}$ and $^{44m}\text{Sc}$ in Nitrogen-Induced Reactions\*

I. R. WILLIAMS AND K. S. TOTH

*Oak Ridge National Laboratory, Oak Ridge, Tennessee*

(Received 2 December 1964)

Thick targets of P, ZnS, and  $\text{CuCl}_2$  were bombarded with 30- to 42-MeV  $^{14}\text{N}$  ions, and excitation functions were obtained for the compound-nucleus reactions with  $^{31}\text{P}$ ,  $^{32}\text{S}$ , and  $^{35}\text{Cl}$  producing  $^{44m}\text{Sc}$ ,  $^{44g}\text{Sc}$ , and  $^{43}\text{Sc}$ . The reaction products were identified by means of their characteristic gamma rays and half-lives, and quantitatively studied by radioactive assay. The data were combined with some previously obtained at  $^{14}\text{N}$  energies below 28 MeV. The isomer ratio  $^{44m}\text{Sc}/^{44g}\text{Sc}$  was found to rise with increasing excitation energy and angular momentum for all three targets. The ratios were compared with compound-nucleus theory as treated by Huizenga and Vandenbosch to test assumptions concerning the multipolarity and multiplicity of the gamma quanta emitted by the final nucleus.

### INTRODUCTION

PHOSPHORUS, zinc sulfide, and copper chloride were bombarded with 30–42-MeV  $^{14}\text{N}$  ions, accelerated in the Oak Ridge Tandem Van de Graaff Accelerator, to produce  $^{44}\text{Sc}$  and  $^{43}\text{Sc}$ . The primary purpose of the investigation was to obtain information about nuclear-structure parameters and the reaction mechanism in the production of  $^{44}\text{Sc}$  by studying the cross-section ratios of the two  $^{44}\text{Sc}$  isomers as a function of excitation energies and angular momenta of the compound nuclei. Other workers have investigated the isomeric-yield ratios of  $^{44}\text{Sc}$  produced in reactions induced by neutrons,<sup>1</sup> protons,<sup>2</sup> alpha particles,<sup>3–5</sup> and oxygen and neon<sup>6</sup> ions. One of the authors (KST) has also obtained excitation functions for  $^{14}\text{N}$  at lower bombardment energies.<sup>7,8</sup> The nuclide  $^{44}\text{Sc}$  is a particularly convenient choice because the gamma rays and annihilation quanta are easily resolved and because of the large difference between the half-lives of the two isomeric states. The metastable state,  $^{44m}\text{Sc}(6+)$  de-excites<sup>9</sup> with the emission of a 0.27-MeV gamma ray and has a half-life of 57.6 h<sup>10</sup>; the ground-state  $^{44g}\text{Sc}(2+)$  decays by positron emission<sup>9</sup> followed by a 1.16-MeV gamma ray and has a half-life of 3.9 h.<sup>10</sup> Information concerning the investigated reactions is summarized in Table I.

### EXPERIMENTAL METHOD

Targets were prepared by compressing zinc sulfide, red phosphorus, and copper chloride under a pressure of 5 tons/in.<sup>2</sup> into brass molds  $\frac{3}{4}$  in. in diameter. These targets, thicker than the range of nitrogen ions, presented a hard uniform surface which did not change under bombardment. Before irradiation great care was taken to make them free of moisture by keeping them in a dessicator. The targets were bombarded in a Faraday-cup assembly and beam currents up to 50 nA were recorded; because of the volatile nature of phosphorus the current on it was limited to 20 nA. Most of the nitrogen ions in the beams were quintuply ionized; their energy was known to  $\pm 100$  keV.

After each bombardment, the target was put in a stainless-steel cup and placed in a 3×3-in. NaI(Tl) crystal  $\gamma$ -ray spectrometer connected to a pulse-amplitude analyzer with up to 800 channels. This system and a 1.5×1.5-in. NaI(Tl) crystal spectrometer with a 256-channel analyzer used for the study of long-lived isotopes had been previously calibrated<sup>7</sup> so that accurate determinations of the gamma-ray energies and intensities could be made. The probable error in the absolute photopeak efficiency is estimated to be 15%. Photopeak

TABLE I. De-excitation modes and  $Q$  values.

Target nucleus	Compound nucleus	Observed nucleus	Particles emitted	$Q$ (MeV)
$^{31}\text{P}$	$^{46}\text{Ti}$	$^{44}\text{Sc}$	$p$	8.94
		$^{43}\text{Sc}$	$pn$	-0.76
			$(2n)^a$	-1.54
$^{32}\text{S}$	$^{46}\text{V}$	$^{44}\text{Sc}$	$2p$	0.08
		$^{43}\text{Sc}$	$n2p$	-9.63
			$(p2n)^a$	-10.41
			$(3n)^a$	-11.19
$^{35}\text{Cl}$	$^{48}\text{Cr}$	$^{44}\text{Sc}$	$\alpha p$	1.95
		$^{43}\text{Sc}$	$\alpha pn$	-7.76
			$(\alpha 2n)^a$	-8.54

\* Particles emitted to form the parent,  $^{46}\text{Ti}$ , of the observed nucleus,  $^{43}\text{Sc}$ . The half-life of  $^{46}\text{Ti}$  (0.6 sec) is short so that the measured yield of  $^{43}\text{Sc}$  includes the  $^{46}\text{Ti}$  yield. The parent of  $^{44}\text{Sc}$ , i.e.,  $^{44}\text{Ti}$ , has a half-life of  $\sim 10^8$  y and is therefore not considered. For the  $^{32}\text{S}$  case  $^{46}\text{V}$ , which presumably must also have a short half-life, is produced by  $3n$  emission and eventually decays into  $^{43}\text{Sc}$ .

\* Research sponsored by the U. S. Atomic Energy Commission under contract with the Union Carbide Corporation.

<sup>1</sup> R. J. Prestwood and B. P. Bayhurst, Phys. Rev. **121**, 1438 (1961).

<sup>2</sup> J. W. Meadows, R. M. Diamond, and R. A. Sharp, Phys. Rev. **102**, 190 (1956).

<sup>3</sup> T. Matsuo and T. T. Sugihara, Can. J. Chem. **39**, 697 (1961).

<sup>4</sup> S. M. Bailey, Phys. Rev. **123**, 579 (1961).

<sup>5</sup> C. Riley, K. Ueno, and B. Linder, Phys. Rev. **135**, B1340 (1964).

<sup>6</sup> V. V. Bredel', B. A. Gvozdev, and V. A. Fomichev, Zh. Eksperim. i Teor. Fiz. **45**, 904 (1963) [English transl.: Soviet Phys.—JETP **18**, 622 (1964)].

<sup>7</sup> E. Newman and K. S. Toth, Phys. Rev. **129**, 802 (1963).

<sup>8</sup> M. E. Wetzen and K. S. Toth, J. Inorg. Nucl. Chem. **25**, 1073 (1963).

<sup>9</sup> D. L. Harris and J. D. McCullen, Phys. Rev. **132**, 310 (1963).

<sup>10</sup> Nuclear Data Sheets, compiled by K. Way *et al.* (Printing and Publishing Office, National Academy of Sciences—National Research Council, Washington, D. C., 1960).

TABLE II. Identifying  $\gamma$  rays and branching ratios.

Isotope	Half-life	$\gamma$ -ray energy (MeV)	Branching ratios (%)
$^{44m}\text{Sc}$	57.6 h	0.27	100
$^{44g}\text{Sc}$	3.9 h	1.16	100
$^{43}\text{Sc}$	3.9 h	0.37	21.5

areas from the photon spectra were measured; corrections were included for decay during and following bombardment. Then, with a knowledge of the beam intensity and its degree of ionization, absolute yields per incident particle were calculated. The identifying half-lives, gamma radiations, and the branching ratios<sup>10</sup> used in calculating the reaction yields are shown in Table II.

### RESULTS

Figures 1, 2, and 3 show the thick-target yields per incident particle as a function of bombarding energy for  $^{31}\text{P}$ ,  $^{32}\text{S}$ , and  $^{35}\text{Cl}$ , respectively. They include the results obtained at energies below 28 MeV and reported by various experimenters<sup>7,8,11</sup> at this Laboratory. The scatter in the experimental points illustrates the relative experimental error; this error arises from uncertainties in beam intensity, counting statistics, and NaI crystal calibration. In their investigation of nuclear reactions induced on  $^{35}\text{Cl}$  Newman and Toth<sup>7</sup> bombarded RbCl and not the  $\text{CuCl}_2$  used in this study. Their yield points were therefore corrected for the differences in stopping

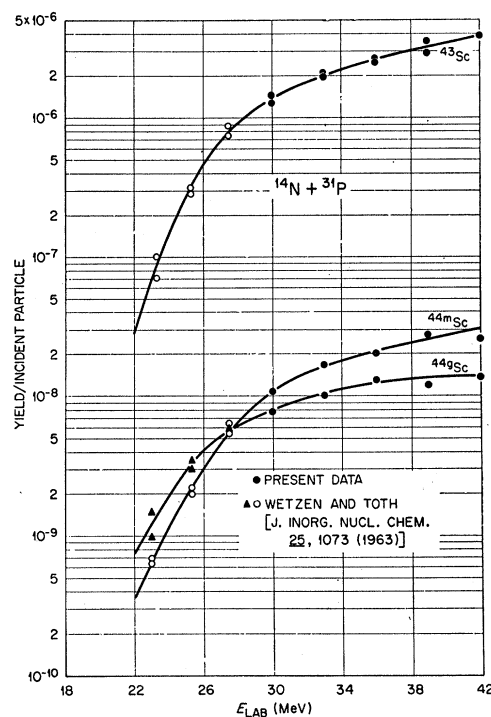


FIG. 1. Yields per incident particle determined for  $^{43}\text{Sc}$ ,  $^{44m}\text{Sc}$ , and  $^{44g}\text{Sc}$  resulting from  $^{14}\text{N}$  bombardment of  $^{31}\text{P}$ .

power, molecular weight, and number of chlorine atoms per molecule between the two target materials before being combined with our data in Fig. 3. From Figs. 1-3, it is clear that the data obtained in the present investi-

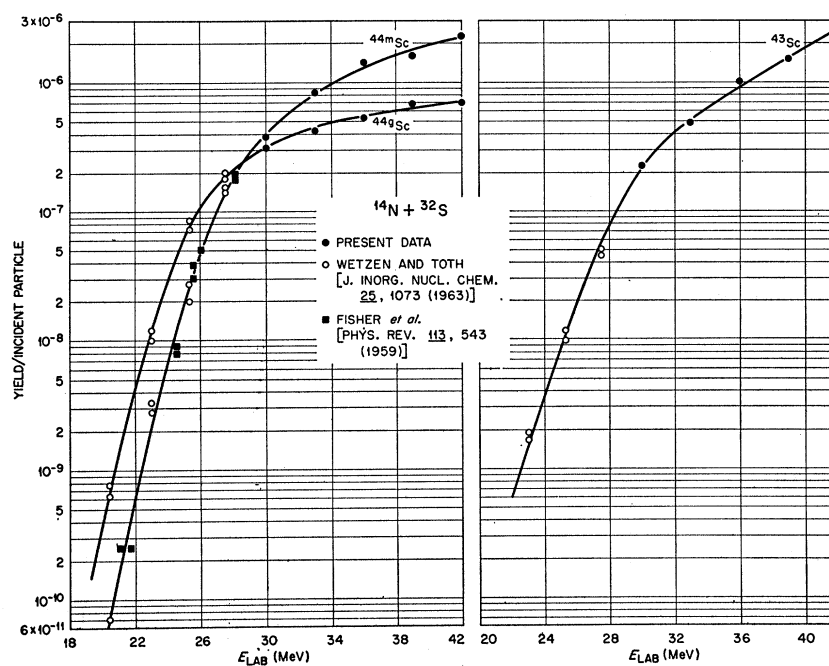


FIG. 2. Yields per incident particle determined for  $^{43}\text{Sc}$ ,  $^{44m}\text{Sc}$ , and  $^{44g}\text{Sc}$  resulting from  $^{14}\text{N}$  bombardment of  $^{32}\text{S}$ .

<sup>11</sup> D. E. Fisher, A. Zucker, and E. Gropp, Phys. Rev. 113, 543 (1959).

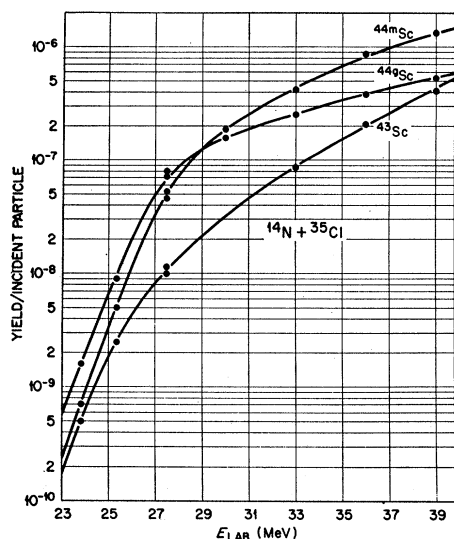


FIG. 3. Yields per incident particle determined for  $^{43}\text{Sc}$ ,  $^{44m}\text{Sc}$ , and  $^{44g}\text{Sc}$  resulting from  $^{14}\text{N}$  bombardment of  $^{35}\text{Cl}$ .

gation are in agreement with the earlier experimental results.

In considering the  $^{35}\text{Cl}$  results one must remember that the reaction products could also be made from  $^{37}\text{Cl}$  by the emission of two additional neutrons. In this process, however, the  $Q$  values are decreased by about 19 MeV. Also, one can compare the yields of  $^{43}\text{Sc}$  and

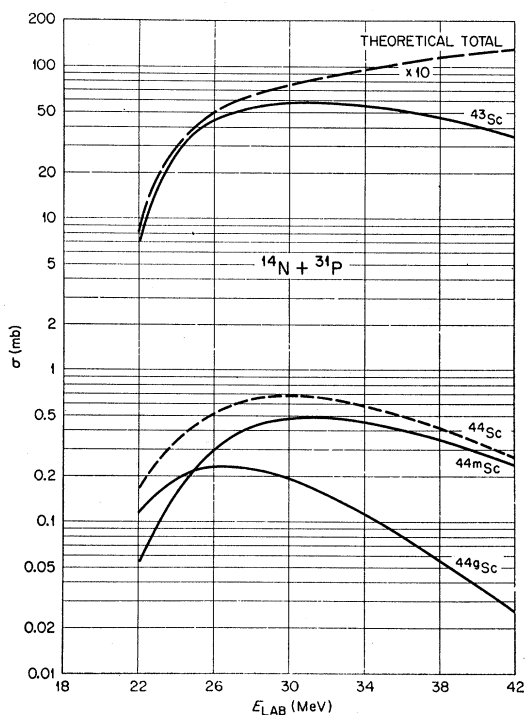


FIG. 4. Excitation functions for reactions induced by  $^{14}\text{N}$  on  $^{31}\text{P}$ . The ordinate scale for the theoretical total cross section should be multiplied by 10.

$^{44}\text{Sc}$  as shown in Fig. 3; the  $^{43}\text{Sc}$  produced in a reaction requiring the emission of an additional neutron has a yield which is substantially less than that of  $^{44}\text{Sc}$ , even at the highest available energy. At the investigated energies the emission of two extra neutrons should lower the yield even more. Finally, it must be remembered that  $^{37}\text{Cl}$  makes up only  $\sim 25\%$  of natural chlorine. Therefore, from the arguments presented above we conclude that at most only a small fraction of the  $^{43}\text{Sc}$  and  $^{44}\text{Sc}$  yields shown in Fig. 3 is due to  $^{37}\text{Cl}$ .

Smooth curves were drawn through each set of experimental points. Cross sections as a function of bombarding energy were calculated from the slopes of these curves. For this determination the stopping powers of each target material for  $^{14}\text{N}$  ions were obtained from

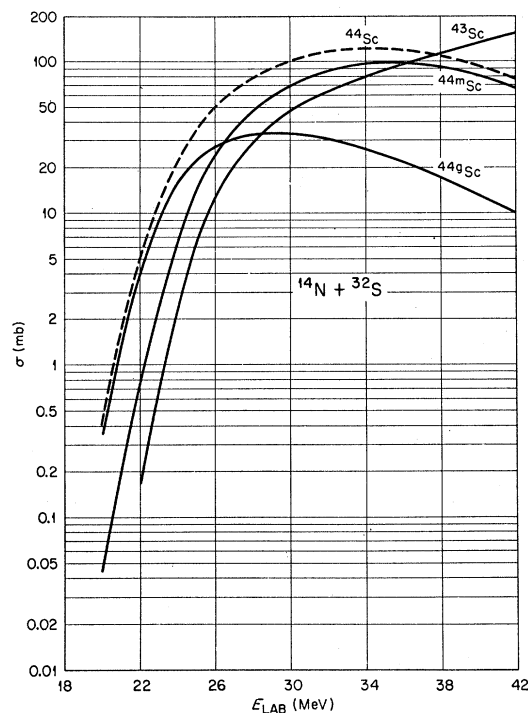


FIG. 5. Excitation functions for reactions induced by  $^{14}\text{N}$  on  $^{32}\text{S}$ .

tabulated data.<sup>12</sup> Excitation functions obtained in this manner are shown in Figs. 4, 5, and 6. The error arising from all sources in the absolute cross sections is estimated to be about  $\pm 30\%$ .

## DISCUSSION

Previous studies<sup>13</sup> of heavy-ion reactions at these bombarding energies indicate that the greatest part of the reaction cross section proceeds in such a way that a number of light particles, protons, neutrons, alpha particles, etc., are emitted and a heavy residual nucleus

<sup>12</sup> L. C. Northcliffe, *Ann. Rev. Nucl. Sci.* **13**, 67 (1963).

<sup>13</sup> A. Zucker, Session D, Report of Paris Conference on Nuclear Physics, 1958 (unpublished).

remains. It is presumed that the reactions investigated here do proceed via this compound nucleus or evaporation mechanism. Otherwise, transfers of very heavy nuclear clusters, e.g.,  $^{13}\text{C}$ , would have to be postulated to explain the observed  $^{44}\text{Sc}$  in this experiment.

In Fig. 7 the isomer ratios (ratio of the formation cross section of  $^{44m}\text{Sc}$  to  $^{44g}\text{Sc}$ ) are displayed. The isomer ratio increases with incident energy for all three reactions as the compound nuclei acquire more angular momentum; thus the final high-spin state of  $^{44m}\text{Sc}$  is populated preferentially over the ground state. One can observe from Fig. 7 that the ratio, over the energy range investigated, is highest for the  $^{31}\text{P}$  reaction and lowest for  $^{35}\text{Cl}$ . Since essentially the same amount of angular momentum is brought into the three systems the difference in the number of particles emitted from the compound nuclei may account for the differences in the isomer ratios. The proton emitted in the  $^{31}\text{P}$  reaction

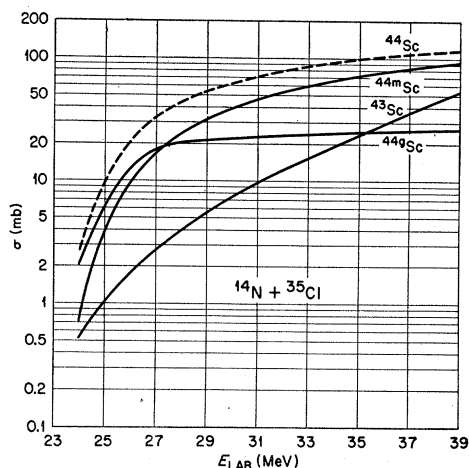


FIG. 6. Excitation functions for reactions induced by  $^{14}\text{N}$  on  $^{35}\text{Cl}$ .

would carry off less angular momentum than the two protons in the  $^{32}\text{S}$  case; these in turn would carry off less than the alpha particle and proton in the  $^{35}\text{Cl}$  reaction. A higher yield of the high-spin isomer would be expected in the system left with more angular momentum. This is consistent with the data shown in Fig. 7. The ratio for  $^{35}\text{Cl}$  seems to increase much less rapidly for energies above 30 MeV. This may be due to the alpha particle taking away proportionately a greater amount of angular momentum as the energy increases. Also, for energies above 30 MeV it becomes energetically possible for more particles to be boiled off and these may take away more angular momentum. Thus, for the evaporation of two protons and a triton the threshold is 25 MeV, for two deuterons and a proton it is 30 MeV, and for three protons and two neutrons it is 36 MeV. Attention must be drawn, however, to the large experimental errors involved in the isomer ratios. If one considers the extreme error limits, the differences in the three isomer ratios become less striking. Finally,

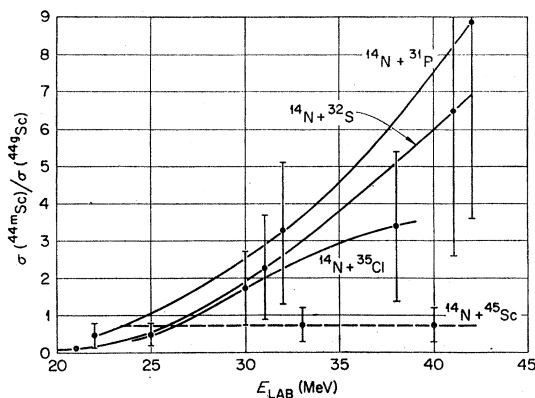


FIG. 7. Isomer ratios as a function of incident energy resulting from the  $^{14}\text{N}$  bombardment of  $^{31}\text{P}$ ,  $^{32}\text{S}$ ,  $^{35}\text{Cl}$ , and  $^{45}\text{Sc}$ .

we have included in Fig. 7 the isomer ratio obtained in the neutron-transfer reaction  $^{45}\text{Sc}(^{14}\text{N},^{15}\text{N})^{44}\text{Sc}$  by Gaedke and Toth.<sup>14</sup> The ratio remains constant with increasing energy, indicating that in the transfer reaction the  $^{44}\text{Sc}$  is left with essentially the same amount of angular momentum over a 20-MeV energy range.

Because of the large number of variables in the theory<sup>15</sup> of the compound-nucleus reaction mechanism a study of the cross sections for a particular reaction does not yield much quantitative data about the structure of the nucleus. When, however, a nuclide has an isomeric state and cross-section measurements are made of its formation in the ground and the excited state, the ratio of the cross sections is more amenable to useful theoretical analysis. This latter three-state theory has been developed by Huizenga and Vandenbosch,<sup>16</sup> and was applied here to  $^{44}\text{Sc}$ . The calculations were performed on a CDC 1604 computer.<sup>17</sup>

High-energy projectiles can bring into a nucleus a whole spectrum of angular momenta; hence the compound nuclei that are produced have a wide distribution of angular momenta. This distribution is given by the following equation<sup>15,17</sup> for the cross section for the formation of a compound nucleus with an angular momentum  $J_c$  when produced by a projectile of energy  $E$ :

$$\sigma(J_c, E) = \pi\lambda^2 \sum_{s=|I-s|}^{I+s} \sum_{l=|J_c-s|}^{J_c+s} \frac{2J_c+1}{(2s+1)(2I+1)} T_l(E), \quad (1)$$

where  $\lambda$  is the de Broglie wavelength of the incoming particle,  $I$  is the intrinsic spin of the target nucleus,  $S$  is the channel spin,  $s$  is the intrinsic spin of the projectile, and  $T_l(E)$  is the barrier transmission coefficient

<sup>14</sup> R. M. Gaedke and K. S. Toth, Oak Ridge National Laboratory (unpublished data).

<sup>15</sup> J. M. Blatt and V. F. Weisskopf, *Theoretical Nuclear Physics* (John Wiley & Sons, Inc., New York, 1952).

<sup>16</sup> J. R. Huizenga and R. Vandenbosch, *Phys. Rev.* **120**, 1305, 1313 (1960).

<sup>17</sup> W. L. Hafner, Jr., J. R. Huizenga, and R. Vandenbosch, Computer Program for Calculating the Relative Yields of Isomers Produced in Nuclear Reactions, Argonne National Laboratory Report ANL-6662, 1962 (unpublished).

for a projectile of angular momentum  $l$  and energy  $E$ . The transmission coefficients for many  $l$  values at several bombarding energies were obtained by means of a computer program LEONORA<sup>18</sup> that utilizes optical-model parameters. Summation of the partial cross sections for the reaction  $^{14}\text{N}+^{31}\text{P}$  yielded the theoretical total formation cross section shown in Fig. 4; total cross sections for the  $^{14}\text{N}+^{32}\text{S}$  and  $^{14}\text{N}+^{35}\text{Cl}$  reactions should have almost the same value.

A nuclear state with angular momentum  $J_e$  can decay by particle emission to final states with a variety of angular-momentum values, each of which are denoted by  $J_f$ . The relative probability for a transition between  $J_e$  and  $J_f$  is given by

$$P(J_f)_{J_e} \propto \rho(J_f) \sum_{s=|J_f-s'|}^{J_f+s'} \sum_{l'=|J_e-s|}^{J_e+s} T_{l'}(E), \quad (2)$$

where  $s'$  is the intrinsic spin of the emitted particle and  $T_{l'}(E)$  is the transmission coefficient of the emitted particle with angular momentum  $l'$  and energy  $E$ . These latter values were also obtained from the LEONORA program. The  $\rho(J_f)$  is the density of levels of spin  $J_f$  and is taken to be of the form<sup>19,20</sup>:

$$\rho(J_f) \propto (2J_f+1) \exp[-(J_f+\frac{1}{2})^2/2\sigma^2], \quad (3)$$

where  $\sigma$  is the spin-cutoff factor. The normalized yield of  $J_f$  is obtained by summing over all values of  $J_e$ , weighted according to Eq. (2). The process is repeated for the emission of succeeding particles.

Because there is a spectrum of energies for the evaporated particles, it is necessary either to use transmission coefficients for the mean energy or to use these for selected energy bins and to weight the results according to the spectrum. Bishop<sup>21</sup> has found that for isomer ratio calculations involving neutron-emission spectra the results obtained by the two methods are virtually the same. Since proton or alpha-particle spectra from compound-nucleus reactions have a Maxwell-Boltzmann distribution modified at the lower energies by Coulomb barrier effects the mean energy is difficult to calculate.<sup>22</sup> Experimentally, the most probable energy value is always found to be near the Coulomb barrier, and so calculations were performed for 5-MeV protons and 7-MeV alpha particles. In addition it was found that the calculated values of the isomer ratios did not change appreciably with energy of emitted particle, especially in the mean energy region. This is shown in Fig. 8 where calculated values of the isomer ratio as a function of proton-emission energy are plotted.

<sup>18</sup> The authors wish to thank R. H. Bassel and R. M. Drisko for making available the IBM-7090 code LEONORA for calculating penetrability factors. Optical-model parameters were supplied by R. H. Bassel.

<sup>19</sup> H. A. Bethe, *Rev. Mod. Phys.* **9**, 84 (1937).

<sup>20</sup> C. Bloch, *Phys. Rev.* **93**, 1094 (1954).

<sup>21</sup> C. T. Bishop, Argonne National Laboratory Report ANL-6405, 1961 (unpublished).

<sup>22</sup> M. A. Preston, *Physics of the Nucleus* (Addison-Wesley Publishing Company, Inc., Reading, Massachusetts, 1962), Chap. 17, p. 534.

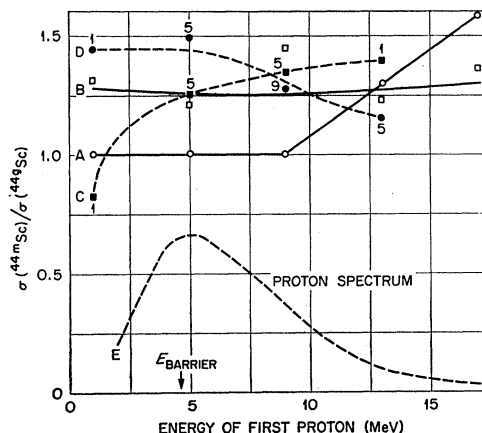


FIG. 8. Variation of the calculated isomer ratio as a function of proton-emission energy. Curve A: 22 MeV  $^{14}\text{N}+^{31}\text{P}$ . Curve B: 42 MeV  $^{14}\text{N}+^{31}\text{P}$  (multiply ordinate scale by 10). Curve C: 22 MeV  $^{14}\text{N}+^{32}\text{S}$ . Curve D: 42 MeV  $^{14}\text{N}+^{32}\text{S}$  (multiply ordinate scale by 10). The energy of the second emitted proton is given above each point in Curves C and D. Curve E: The assumed proton-evaporation spectrum following 42-MeV  $^{14}\text{N}$  bombardment.

Curves A and B are for  $^{14}\text{N}+^{31}\text{P}$  at 22 and 42 MeV (lab), respectively, and curves C and D are for  $^{14}\text{N}$  and  $^{32}\text{S}$  at 22 and 42 MeV, respectively. The numbers in parenthesis along curves C and D are the energies in MeV of the second evaporated proton. Curve E is the estimated proton evaporation spectrum following 42-MeV  $^{14}\text{N}$  bombardment.

If it is assumed that de-excitation by electromagnetic radiation occurs only after particle emission, then it is feasible to calculate the final angular-momentum distribution quite simply. The probability of decaying from a state  $J_f$  to a state  $J_{f'}$  is assumed to be proportional only to the density of final states with spin  $J_{f'}$ . The total normalized yield  $J_{f'}$  is given by the formula

$$P_{J_{f'}} = \frac{\sum_{J_f=|J_{f'}-l|}^{J_{f'}+l} P_{J_f} \rho(J_{f'}) \delta_{J_f J_{f'}}}{\sum_{J_f=|J_{f'}-l|}^{J_{f'}+l} \rho(J_{f'})}, \quad (4)$$

where  $\rho(J_{f'})$  is defined as in (3),  $l$  is now the multipolarity of the gamma quanta and  $P_{J_f}$  is the normalized initial angular-momentum distribution following evaporation of the last particle.

For the reaction  $^{14}\text{N}+^{35}\text{Cl}$  the angular-momentum distribution of the compound nucleus before and after successive emission of an alpha particle, a proton, and four photons is shown in Fig. 9. It shows that though alpha particles take away more angular momentum than protons and photons the difference is not very great. Because of this the predicted isomer ratios for reactions involving  $^{31}\text{P}$ ,  $^{32}\text{S}$ , and  $^{35}\text{Cl}$  do not differ much one from another when the same parameters are employed.

The theoretical value of the isomer ratio was obtained by assuming that there is a sharp cutoff value of the final nuclear angular momentum, e.g.,  $J_{f'}=k$ , below which states de-excite to the ground state, and

above which states de-excite to the isomeric state. With this assumption the ratio was then predicted by summing the partial cross sections above and below  $k$  and dividing the high-spin part by the low-spin part.<sup>23-25</sup> Because the isomeric and ground state of  $^{44}\text{Sc}$  very probably have spin values 6 and 2, respectively, it was assumed that the spin state 4 divides equally in the final gamma-ray transition to the ground and excited states:

$$\text{ratio} = \sum_5^{\infty} (P_{J,J'} + 1/2P_4) / \sum_{J,J'=0}^3 (P_{J,J'} + 1/2P_4). \quad (5)$$

The average energy of gamma rays of multipolarity  $l$  in the cascade from the residual nucleus can be calculated from an equation due to Strutinski *et al.*<sup>26</sup>:

$$\bar{E}_\gamma \simeq (2l+2)(E_c/a)^{1/2}. \quad (6)$$

Vandenbosch and Haskin<sup>27</sup> have modified the equation slightly for dipole radiation so

$$\bar{E}_\gamma = [4(E_c - 1)/a]^{1/2}, \quad (7)$$

where  $E_c$  is the excitation energy. The parameter  $a$  is a function of the mass number and was taken<sup>28</sup> to be  $(A/10) \text{ MeV}^{-1}$ . To test whether the values of the parameter  $a$  are suitable, a nuclear-evaporation computer program (EVAP)<sup>29</sup> using a Monte Carlo calculation (based upon the work of Dostrovsky *et al.*<sup>30</sup>) was utilized to predict the relative number of nucleons and alpha particles evaporated. This was done for  $^{14}\text{N}$  incident on  $^{31}\text{P}$  and  $^{32}\text{S}$  for energies from 22 to 42 MeV in batches of 1000 case histories each with different values of the parameter  $a$  ranging from 1 to 10. The ratio of the number of  $^{43}\text{Sc}$  to  $^{44}\text{Sc}$  nuclei thus obtained was compared with experiment, and reasonable agreement was found for the above choice of value for  $a$ .

The number of gamma rays emitted was estimated in four different ways:

(a) Equation (7) was employed for dipole radiation to calculate  $\bar{E}_\gamma$ . After emission of a photon with that energy the excitation of the nucleus would be reduced to  $E_c - \bar{E}_\gamma$ . This value was used to calculate the energy of the second photon, the procedure repeated until the

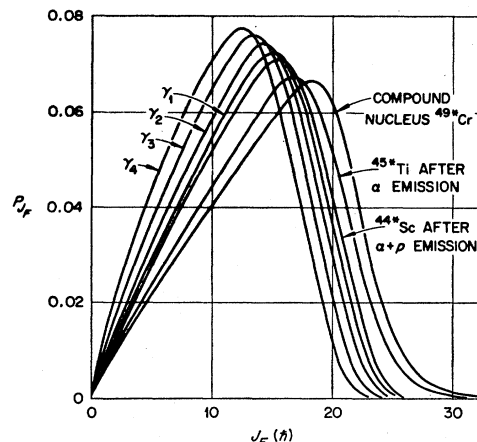


Fig. 9. Angular momentum distributions of the compound-nucleus  $^{48}\text{Cr}$  (formed by 42-MeV  $^{14}\text{N}$  bombardment of  $^{36}\text{Cl}$ ), the nucleus after emission of a 7-MeV alpha particle, a 5-MeV proton, and then 4-dipole photons.

remaining excitation energy was 1 MeV or less, then a single additional photon was assumed to be emitted. For each excitation energy an appropriate spin-cutoff factor was employed, as explained below.

(b) Equation (6) was employed for quadrupole radiation and the above procedure yielded gamma rays whose energy decreased with the remaining excitation energy.

(c) Mollenauer<sup>31</sup> has found experimentally that the gamma rays have a distribution such that their average energy is  $1.2 \pm 0.3 \text{ MeV}$ . Even though this result was found at very different energies and for much heavier mass targets than the present measurements, it was thought that it would be interesting to divide the total excitation energy by 1.2-MeV to obtain the average number of emitted dipole and quadrupole gamma rays.

(d) The same was repeated for equal-energy dipole gamma rays of 2 MeV since gamma transitions of this character are predicted by a Fermi-gas model of an excited nucleus.<sup>25</sup>

Figures 10, 11, and 12 show the comparison between the calculated values of the isomer ratio, as a function of energy for the five assumptions, and the experimental results. No single curve gives good agreement between experiment and theory over the whole energy range, but the closeness is sufficient to indicate that the use of the approach due to Huizenga and Vandenbosch is essentially correct.

In addition to the multipolarity and multiplicity of electromagnetic radiation, the value of the spin density parameter  $\sigma$  is a variable in the calculations of isomer ratios. It appears in the expression for the level density [Eq. (4)] that is involved in the second (particle-emission) and third (photon-emission) stages of the calculations.

<sup>31</sup> J. F. Mollenauer, thesis, Lawrence Radiation Laboratory Report UCRL-9724, 1960 (unpublished); Phys. Rev. 127, 867 (1962).

<sup>23</sup> L. Katz, L. Pease, and H. Moody, Can. J. Phys. 30, 476 (1952).

<sup>24</sup> D. W. Seegmiller, Lawrence Radiation Laboratory Report UCRL-10850, 1963 (unpublished).

<sup>25</sup> R. L. Kiefer, Lawrence Radiation Laboratory Report UCRL-11049, 1963 (unpublished).

<sup>26</sup> V. M. Strutinski, L. V. Grosheer, and M. K. Akimora, Nucl. Phys. 16, 657 (1960).

<sup>27</sup> R. Vandenbosch and L. Haskin, Argonne National Laboratory (unpublished) quoted in Refs. 24 and 25.

<sup>28</sup> J. M. B. Lang and K. J. LeCouteur, Proc. Phys. Soc. (London) A67, 586 (1954).

<sup>29</sup> L. Dresner, Oak Ridge National Laboratory Report, ORNL-TM-196, 1961 (unpublished), modified by E. Newman to enable the inclusion of a  $E^{-2}$  term in the level density expression.

<sup>30</sup> I. Dostrovsky, Z. Fraenkel, and G. Friedlander, Phys. Rev. 116 683 (1959); I. Dostrovsky, Z. Fraenkel, and L. Winsberg, *ibid.* 118, 781 (1960); I. Dostrovsky, Z. Fraenkel, and P. Rabino-witz, *ibid.* 118, 791 (1960).

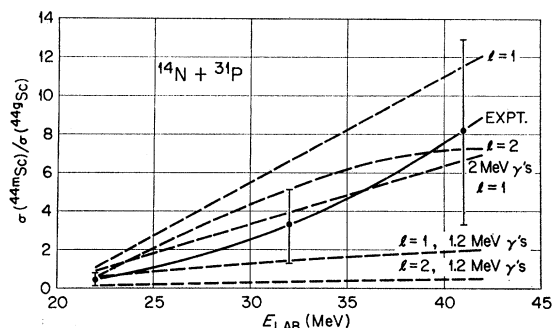


FIG. 10. Theoretical and experimental isomer ratios for the reaction  $^{14}\text{N} + ^{31}\text{P}$ ;  $\sigma = \sigma_r$ .

It has been shown<sup>24,25</sup> that  $\sigma$  is related to the nuclear moment of inertia and the nuclear temperature through an equation of state of the nuclear matter. The way in which  $\sigma$  varies with excitation energy of a nucleus depends on the nuclear model employed. Three models were considered using formulas quoted by Seegmiller<sup>24</sup>

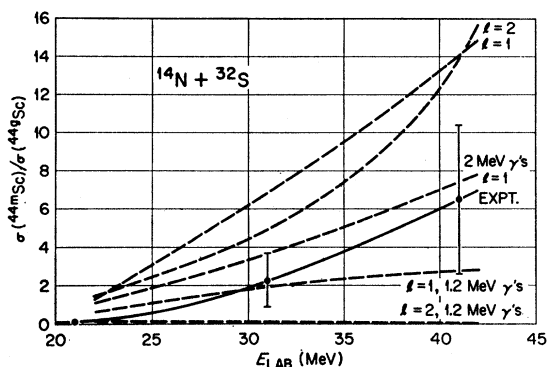


FIG. 11. Theoretical and experimental isomer ratios for the reaction  $^{14}\text{N} + ^{32}\text{S}$ ;  $\sigma = \sigma_r$ .

and Kiefer.<sup>25</sup> For the Fermi-gas model the spin-density parameter slowly increases from 3 to 5.5 with excitation energy from 5 to 60 MeV. The moment of inertia of a rigid sphere is used to calculate the spin-density parameter in the Fermi-gas model; therefore the  $\sigma$  determined by means of this model is usually designated by  $\sigma_r$ . For the superconductor model  $\sigma$  was found to be about 5%

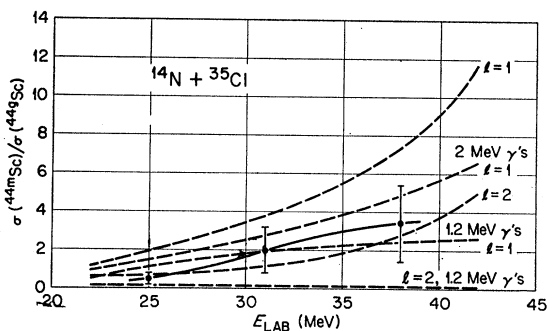


FIG. 12. Theoretical and experimental isomer ratios for the reaction  $^{14}\text{N} + ^{35}\text{Cl}$ ;  $\sigma = \sigma_r$ .

smaller than  $\sigma_r$  over most of the energy range. The Fermi-gas model with pairing interactions yielded a  $\sigma$  which was approximately 15% lower than  $\sigma_r$ . Owing to the large errors in the experimentally determined isomer ratios, it was clear that the data could not be used to make a choice between ratios calculated by utilizing values of  $\sigma$  that differ from one another by such small amounts. Computations were therefore performed with spin-density parameter values of  $0.66\sigma_r$ ,  $\sigma_r$ , and  $1.33\sigma_r$ . The family of isomer ratio curves for the  $^{14}\text{N} + ^{31}\text{P}$  reaction are given in Figs. 13, 10, and 14, respectively. No consistent agreement is achieved between experiment

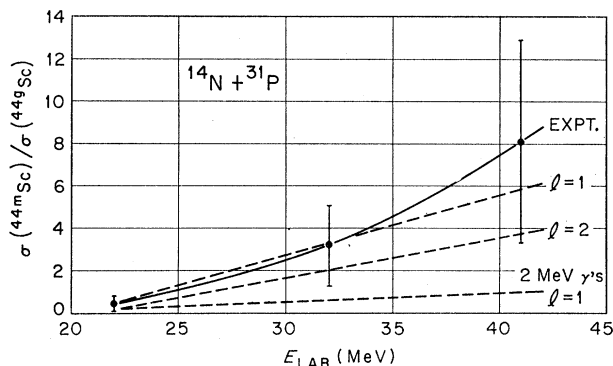


FIG. 13. Theoretical and experimental isomer ratios for the reaction  $^{14}\text{N} + ^{31}\text{P}$ , using  $\sigma = 0.66 \sigma_r$ .

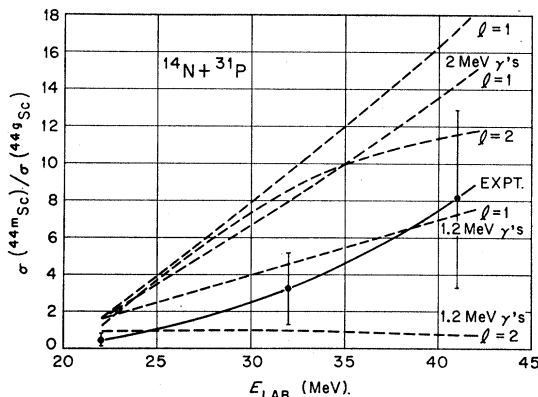


FIG. 14. Theoretical and experimental isomer ratios for the reaction  $^{14}\text{N} + ^{31}\text{P}$ , using  $\sigma = 1.33 \sigma_r$ .

and theory. Curves obtained for  $^{14}\text{N}$  bombardment of  $^{32}\text{S}$  and  $^{35}\text{Cl}$  show similar features. We are thus unable to say which of the three nuclear models best fits the facts.

ACKNOWLEDGMENTS

The authors wish to thank M. L. Halbert and A. Zucker for their helpful comments. They also wish to thank R. H. Bassel for supplying the optical-model parameters to calculate penetrability factors and E. Newman for the use of his modified EVAP program. The cooperation of the Tandem Van de Graaff crew is gratefully acknowledged.